



ハノイ市における繊維質材料混合流動化処理土の埋戻し地盤への適用に関する研究

メタデータ	言語: eng 出版者: 公開日: 2015-12-22 キーワード (Ja): キーワード (En): 作成者: ズウオン, クワン フン メールアドレス: 所属:
URL	https://doi.org/10.15118/00005132

Deformation and Strength Characteristics of Liquefied Stabilized Soil (LSS) Evaluated by Laboratory Testing

3.1 INTRODUCTION

It is well known that since LSS is one of the cement-treated soils, strength property indicates more brittle behavior when the strength increases as increasing an amount of cement stabilizer. To improve the brittle characteristic of LSS, Kohata et al. (2002, 2004, and 2007) have considered on a reinforcement method by mixing crushed waste newspaper as a fiber material into LSS, and carried out a series of unconfined and triaxial compression tests. The results indicated that by the reinforcement effect, the brittle property of LSS mixed with fiber material after the peak in $q\sim\varepsilon_a$ curve was improved. However, influence of time-dependency on strength and deformation characteristics of LSS mixed by fibered material have been not evaluated. Moreover, an investigation on LSS reinforced by the fiber material placed in-situ has been not performed, and then, the difference of strength and deformation property is not found well between a specimen retrieved by block sampling at in-situ ground and a specimen prepared in laboratory. In this chapter, two experimental works were carried out separately to investigate these characteristics of LSS mixed with fibered material. The first one was conducted to evaluate the time-dependency on deformation property of LSS mixed with fibered material, and the second one was performed to investigate the strength and deformation characteristics of LSS reinforced by fiber material prepared at laboratory and field. The test results were discussion and the characteristics of LSS mixed with fibered material were evaluated.

3.2 TIME-DEPENDENCY ON DEFORMATION PROPERTY OF LSS

In this section, influence of time-dependency on strength and deformation characteristics of LSS mixed by fibered material was investigated. There are two different components of the time effect (Tatsuoka et al., 2002) as shown in Figure 3.1 and Figure 3.2, respectively. Aging effects are defined as time-dependent changes in the intrinsic stress-strain properties, including peak strength, elasticity, yielding and viscosity such as cementation, weathering. The aging effect can be expressed as a function of the time (t_c) having specially defined. Loading rate effects are defined as the strain rate-dependency of stress-strain behavior due to the viscous property, typically noted by creep deformation and strain rate effect on stress-strain behavior. The viscous property is a function of instantaneous irreversible (or visco-plastic) strain rate ($\dot{\epsilon}$) and other relevant parameter, not by time. Recently, the researches on time-dependent shear deformation characteristics of geomaterials have been reported (Tatsuoka et al., 2002; Di Benedetto et al., 2002). However, the characteristics of LSS mixed with fibered material haven't been known (Koyama et al., 2012). Therefore, this study aims to investigate the time-dependency on shear deformation characteristics of LSS mixed with fibered material. A series of specimens was subjected to $\bar{C}\bar{U}$ tests which was isotropically consolidated under effective confined pressure of 98 kPa and subjected to triaxial compression tests (TC tests) under four different conditions of axial strain rate, respectively.

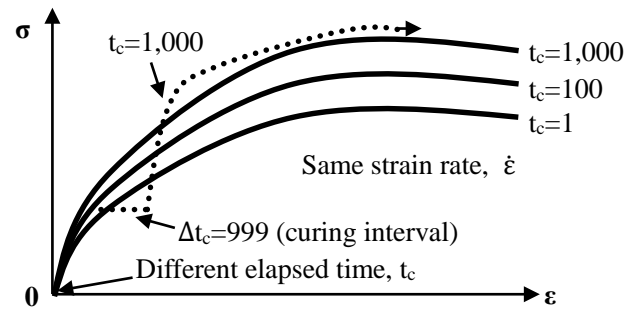


Figure 3.1 Aging effect on stress-strain

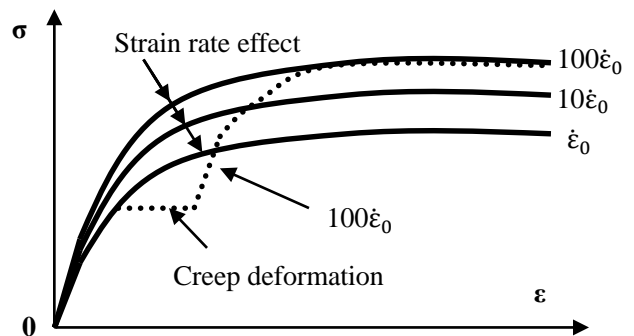


Figure 3.2 Loading rate effect on stress-strain relation

3.2.1 Test procedure

3.2.1.1 Test material

In this study, NSF-CLAY was used as a base material. The physical properties are shown in Table 1. The cement stabilizer was used a special cement type, namely Geoset 200 made by Taiheiyo Cement Co. The fiber material was used crushed newspaper.

Table 3.1 Physical Properties of NSF-CLAY

Density of particle ρ_s (g/cm ³)	2.762
Liquid limit W_L (%)	60.15
Plastic Limit W_p (%)	35.69
Plasticity Index I_p	24.46

3.2.1.2 Mixing method

In general, there are two LSS mixing methods used for excavated soil containing a large quantity of fine particles, which are slurry type and adjustment slurry type. In this study, the slurry type was used due to easier preparation. In this method, water was added moderately to soil for adjusting density of slurry, then the cement stabilizer was added and mixed.

A series of mixing tests were carried out by changing density of slurry and amount of cement stabilizer. The bleeding rate, flow value and unconfined compressive strength were determined by soil tests for each of LSS at curing time of 28 days. The values thus obtained were to present a standard mix proportion for this study.

3.2.1.3 Specimen preparation

Based on the standard mix proportion design figure (Kohata et al., 2011), in this study, the bleeding rate was less than 1 %, the content of cement stabilizer was 80 kg/m³ and the target density of LSS was 1.280 g/cm³.

LSS was prepared by mixing cement stabilizer into slurry in a hand mixer to adjust the density. The density test was performed by measuring the mass of slurry filled into stainless steel container of 400 cm³ called "AE mortar container". After obtaining the target density, the fibered material was added to and mixed carefully by hand mixer. The flow test was conducted in accordance with JHS A313 – Japan Highway Public Corporation Standard “Testing Method for Air Mortar and Air Milk, 1.2 cylinder sample” in order to determine the liquidity of LSS. To remove air bubble trapped in LSS, the vacuum pressure of 98 kPa was applied to sample for 30 minutes. Then the fresh LSS was placed into mould of 5 cm in diameter and 10 cm in height, the top surface of the specimen was cover with polymer film. Finally, the LSS samples mixed with fibered material content of 0, 20 kg/m³ were cured under air humidity and indoor temperature of 20±3°C for 28 and 56 days, respectively.

3.2.1.4 Test method and equipment

The outline of apparatus for triaxial compression tests is shown in Figure 3.3. To avoid the effects of bedding error caused at the lubricated top and bottom ends of the specimen, a pair of Local Deformation Transducer (LDTs) (Goto et al., 1991) was set on the lateral surface of a specimen to measure axial displacement. When value of LTD exceeds a measurable range, axial displacement was used value of proximeter and dial gauge by correcting the bedding error. In these tests, a digital servo motor, which enable to control axial displacements with high precision, and can ignore backlash when

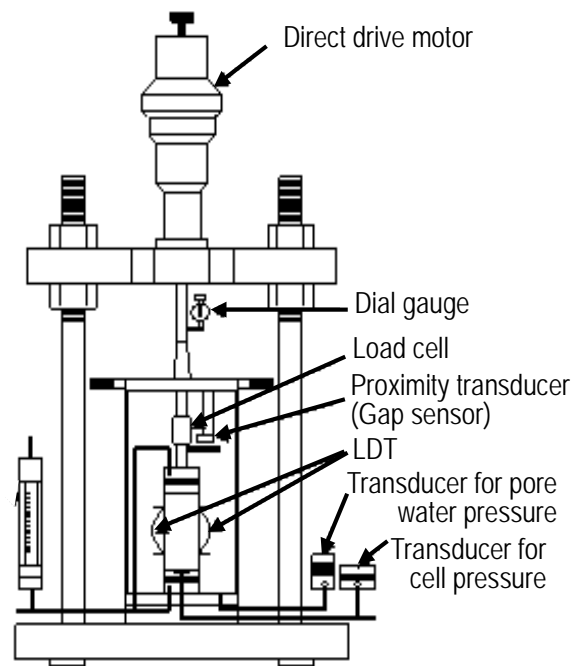


Figure 3.3 Schematic of CUB test apparatus

reversing the loading direction, was used for loading device. The whole operation of apparatus during the test was automatically controlled by a computer program.

The \overline{CU} tests were performed for 28 and 56 days cured specimens, respectively. Saturation of specimen was achieved by double vacuum pressure method that have de-aired water flowed through specimen under back pressure of 196 kPa. After isotropically consolidated during 12 hours under effective confined pressure of 98 kPa, the specimen was subjected to triaxial compression process. To investigate the time-dependency on shear deformation characteristic of LSS mixed with fibered material, four cases of axial strain rate have been applied to triaxial compression process, which is shown in Table 3.2. Case 1 was basic constant rate of 0.054 %/min ($\dot{\epsilon}_0$). Case 2 was 0.54 %/min ($10\dot{\epsilon}_0$). Case 3 was obtained by varying the axial strain rate by 10 times ($\dot{\epsilon}_0 \rightarrow 10\dot{\epsilon}_0 \rightarrow \dot{\epsilon}_0$). During loading at constant rate of axial strain, case 4 was obtained by applying creeps before changing axial strain rate. In addition, the axial strain rate change was carried out in a range of about $\epsilon_a=1\%$.

Table 3.2 Test conditions of axial strain rate

Case 1	0.054 % min ($\dot{\epsilon}_0$)
Case 2	0.54 % min ($10\dot{\epsilon}_0$)
Case 3	$\dot{\epsilon}_0 \rightarrow 10\dot{\epsilon}_0 \rightarrow \dot{\epsilon}_0$
Case 4	$\dot{\epsilon}_0 \rightarrow C \rightarrow \dot{\epsilon}_0 \rightarrow C \rightarrow 10\dot{\epsilon}_0 \rightarrow C \rightarrow \dot{\epsilon}_0$ ※Creep applied before rate change

3.2.2 Test results and discussion

3.2.2.1 Relationship between deviator stress and axial strain

Figure 3.4(a) and (b) show the relationship between deviator stress $q (= \sigma_1 - \sigma_3)$ and axial strain ϵ_a in range of 0~1.4 % from \overline{CU} test under confining pressure $\sigma'_c=98$ kPa of LSS mixed by fibered material content of 0, 20 kg/m³ (Pc-0, 20) at 56 days. TC tests were performed under case 1~case 4, respectively. It is seen that the remarkable different deviator stress q_{max} is not observed for all case regardless addition of fibered material and condition of creep and non-creep during loading.

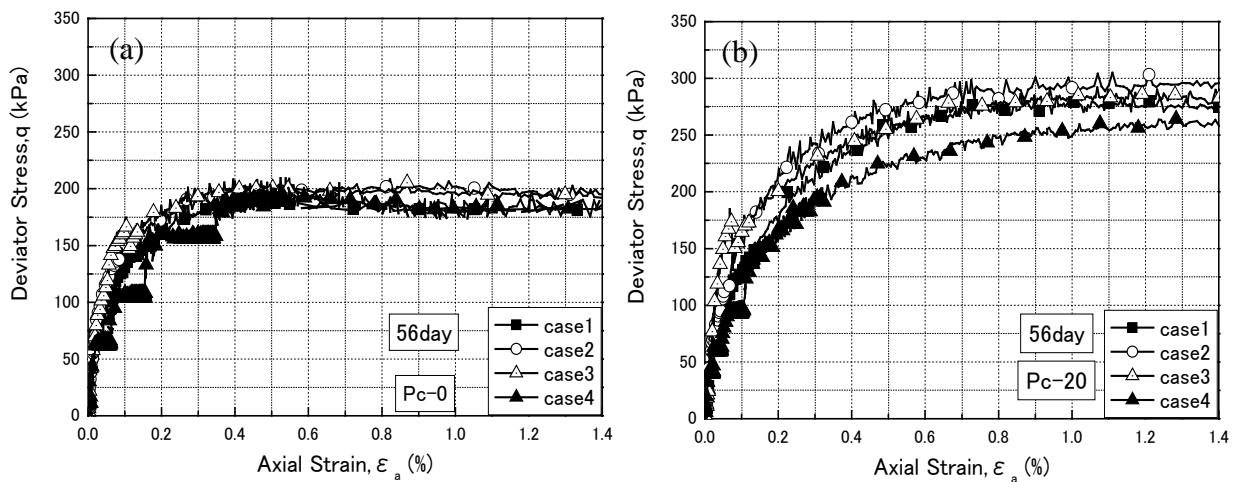


Figure 3.4 $q \sim \epsilon_a$ relation for all cases

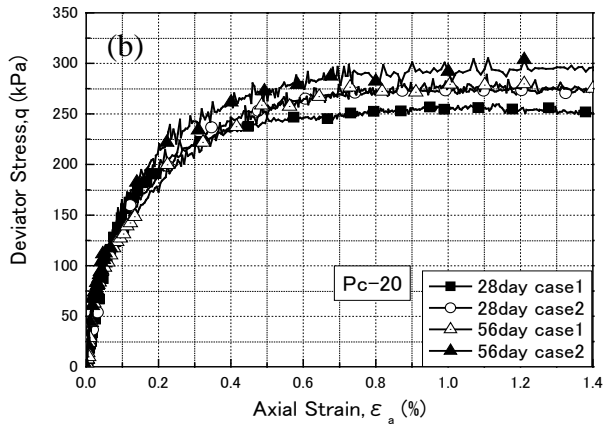
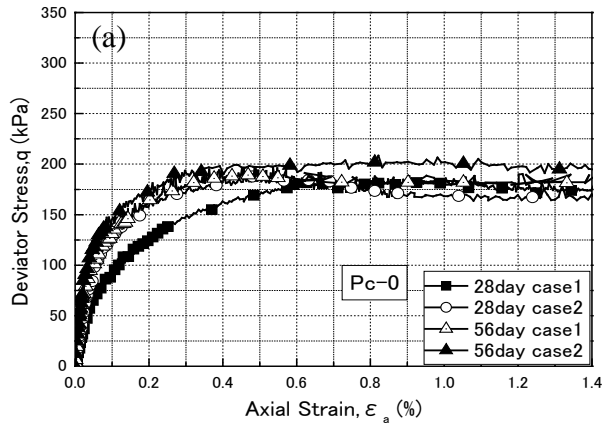


Figure 3.5 $q \sim \epsilon_a$ relation for case 1, 2

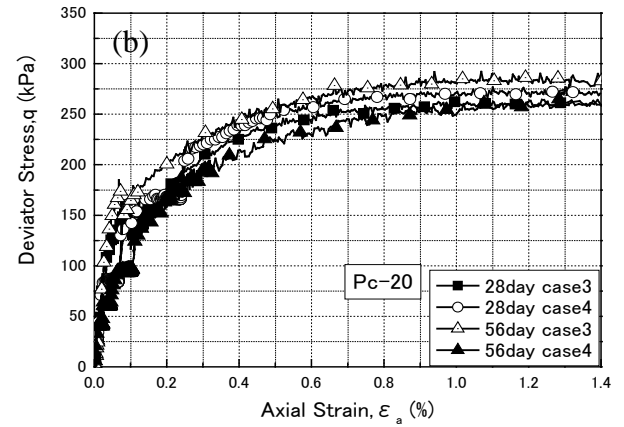
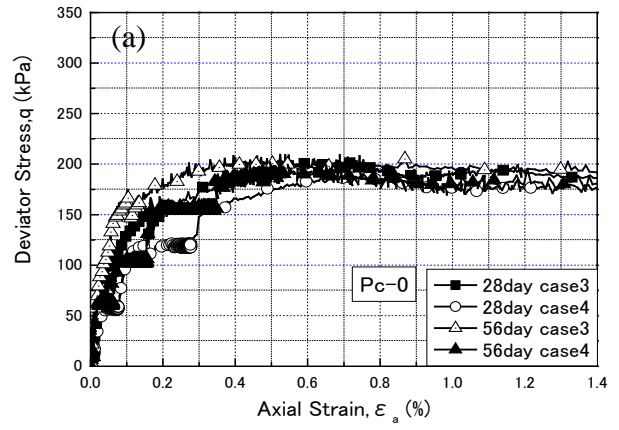


Figure 3.6 $q \sim \epsilon_a$ relation for case 3, 4

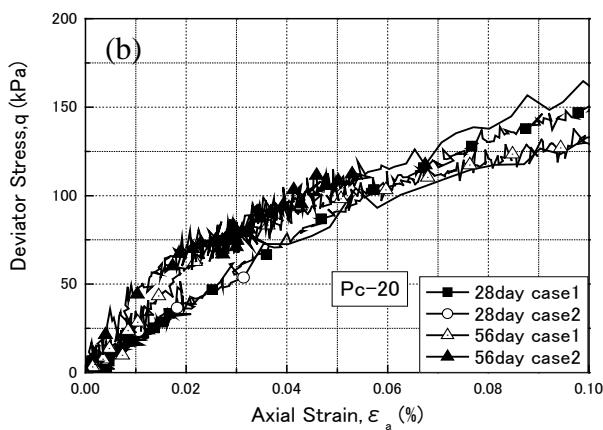
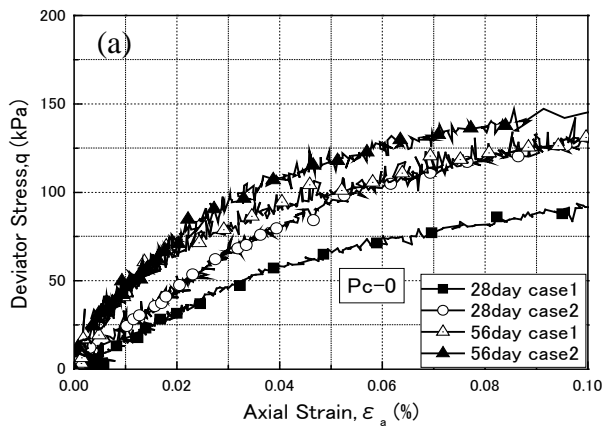


Figure 3.7 $q \sim \epsilon_a$ relation at small strain for case 1, 2

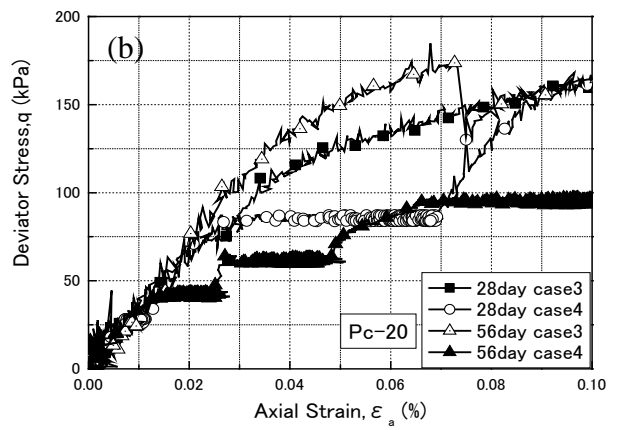
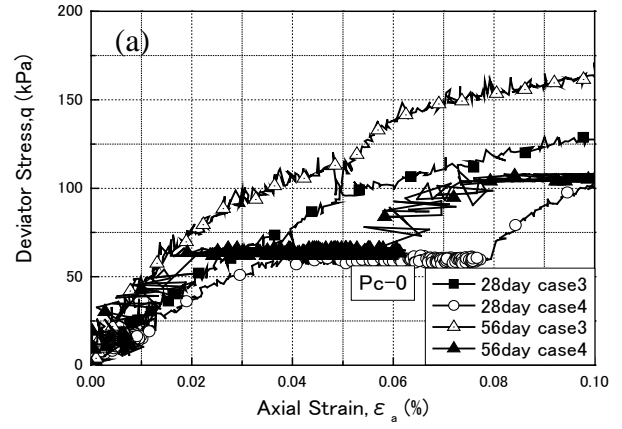


Figure 3.8 $q \sim \epsilon_a$ relation at small strain for case 3, 4

Figure 3.5 and 3.6 show $q\sim\varepsilon_a$ curves for case 1, 2 and case 3, 4 respectively of Pc-0, 20 at 28 days in comparison with that at 56 days. The q_{max} is showing to be no significant difference depending on curing days. In addition, after the peak the curves gradually converge and essentially keep constant, it means that the strength behavior after that is not dependent on number of curing day and axial strain rate. To clear the effect of number of curing day, the more results are shown in Figure 3.7 and 3.8 which respectively show $q\sim\varepsilon_a$ relationship in range of $\varepsilon_a = 0\sim 1.0\%$ for case 1, 2 and case 3, 4 of Pc-0, 20 at 28, 56 curing days. From results of Pc-0, regardless the axial strain rate, the deviator stress at 56 days increase faster as compared with that at 28 days and the tendency is greater as higher strain rate. It is attributed strength development with curing period of the cementing material in LSS. In the results of Pc-20, it indicates that there is no great difference in stress increase regardless the number of curing day. It is considered that the cementation was expected to be delayed due to addition of the fibered material in LSS, thus the $q\sim\varepsilon_a$ curve of Pc-0 that is pure LSS, an increase in the number of curing day resulted in an increase in initial stiffness. However, within the scope of this study, it is considered that at different curing days, a large difference is essentially not seen in the stress increase for the same amount of axial strain increment.

3.2.2.2 Deformation property

a) Definition of Young's modulus

Figure 3.9 shows the definitions of various Young's moduli. The initial Young's modulus E_0 is defined as initial stiffness at small strain of $\varepsilon_a = 0.002\%$ or less. The tangent Young's modulus E_{tan} is defined as tangential gradient in $q\sim\varepsilon_a$ curve, it indicates the non-linearity of deformation property in $q\sim\varepsilon_a$ relation (Kohata et al., 1997, 1999).

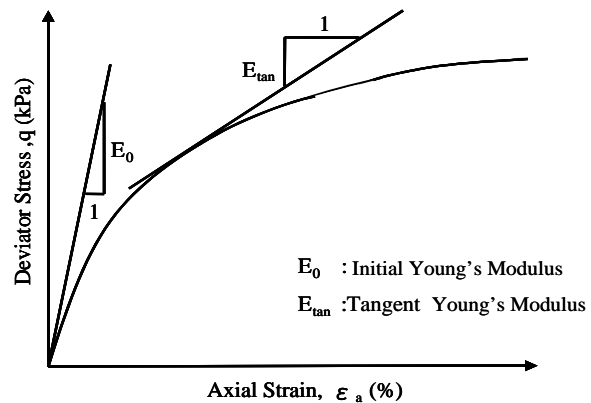


Figure 3.9 Definition of various Young's moduli

b) Initial Young's modulus E_0

The values of E_0 of Pc-0, 20 for each case at 28, 56 days are given in Table 3.3. It is shown that in Pc-0, E_0 of 56 days is greater than that of 28 days. On the other hand, there are slight variations in E_0 of Pc-20. However, increase tendency at 56 days is not seen. Moreover, at 56 days, decrease tendency of E_0 is seen. By the addition of fibered material, as discussed above, it is considered that the progress of cementation was delayed and thus the initial stiffness had been decreased.

Table 3.3 Initial Young's modulus E_0 (MPa)

28 days	Case	Case	Case	Case
Pc-0	270	286	303	317
Pc-20	330	318	424	358
56 days				
Pc-0	505	448	529	515
Pc-20	292	348	310	295

c) Tangent Young's modulus E_{tan}

Figure 3.10(a) and (b) show relationship between E_{tan}/E_0 and q/q_{max} of Pc-0, 20 respectively at 28 days and 56 days for case 1 and case 2. The values were obtained from the $q\sim\varepsilon_a$ curve of \overline{CU} tests under confining pressure of 98 kPa. In Pc-0 specimens that is pure LSS, it is shown that a reduction rate of E_{tan}/E_0 decrease as increasing of curing days. This is due to progress of cementation with curing days. Generally, in the case of cement treated soils, it is reported that nonlinearity of stress-strain curve decreases as increasing of curing days (JGS, 2005). However, in the case of Pc-20, a reduction rate of E_{tan}/E_0 at 56 days increases as compared to 28 days specimens. Therefore, it seems that nonlinearity increases as increasing of curing time by adding fibered material to LSS. For this result, it is considered to conduct further works in the coming time.

Figure 3.11(a) and (b) show relationship between E_{tan}/E_0 and q/q_{max} for case 3 and case 4. In case of Pc-0, it indicates that immediately after a strain rate change as well as a creep stage, E_{tan}/E_0 suddenly increases significantly regardless the curing days, thereafter under loading the reduction of E_{tan}/E_0 tends to be large. Thus there is a tendency that the rigidity is temporarily increased soon after strain rate changes or creep stages. Meanwhile, in case of Pc-20 with similar testing conditions, the range of indicating E_{tan}/E_0 value of 1.0 tends to be larger. Therefore, it is considered that the range of linear in $q\sim\varepsilon_a$ relationship under such conditions becomes large by the addition of fibered material to LSS independently of the curing days.

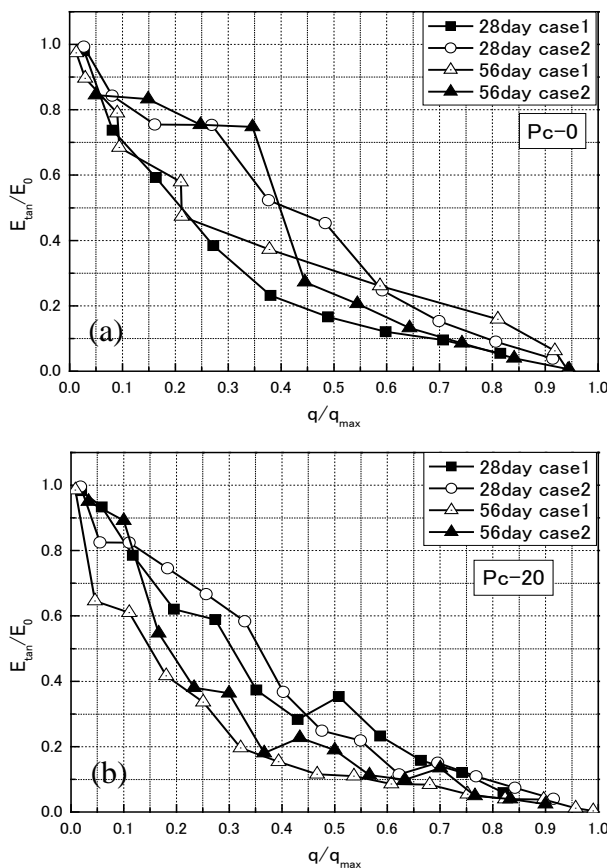


Figure 3.10 $E_{tan}/E_0\sim q/q_{max}$ relation for case 1, 2

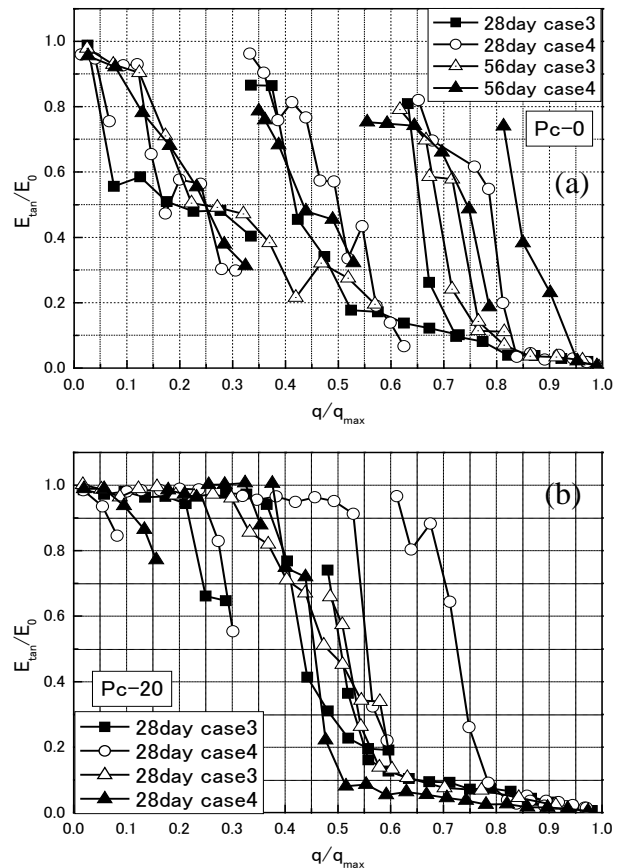


Figure 3.11 $E_{tan}/E_0\sim q/q_{max}$ relation for case 3, 4

d) Strain level-dependency of tangent Young's modulus, E_{tan}

Figure 3.12(a) and (b) show the strain level-dependency on tangent Young's modulus E_{tan} of Pc-0, 20 respectively at 28 days and 56 days for case 1 and case 2. The values of E_{tan} were obtained from the $q \sim \epsilon_a$ curve of \overline{CU} test under confining pressure of 98 kPa. In case of Pc-0, the results indicate that the initial stiffness at 56 days is larger than that at 28 days. In addition, reduction rate of E_{tan} in case 2 is slightly smaller as compared with case 1. It is considered that the stiffness tends to be slightly larger in shearing before the peak in $q \sim \epsilon_a$ curves by increasing the axial strain rate. On the other hand, in case of Pc-20 $E_{tan} \sim \log \epsilon_a$ relationship of 56 days and 28 days is approximately equal. Thus, the initial stiffness is higher for LSS mixed by fibered material with 28 days cured specimens, whereas in 56 days specimens, that is lower. This is suggested that progress of cementation is delayed by addition of fibered material, and thus it causes a decrease of rigidity in small strain level. For this result, it is considered to conduct further works in the coming time.

Figure 3.13(a) and (b) show the strain level-dependency on tangent Young's modulus E_{tan} of Pc-0, 20 respectively at 28 days and 56 days for case 3 and case 4. In case of Pc-0, in large range of shear strain level, E_{tan} temporarily increases significantly by giving strain rate changes or creep actions. Meanwhile, for the results of Pc-20, it is seen that E_{tan} increases nearly to E_0 and the range is larger. Thus, the rigidity during loading before the peak in $q \sim \epsilon_a$ relationship increases temporarily in a large strain level after a creep stage and a change of strain rate independently of curing days.

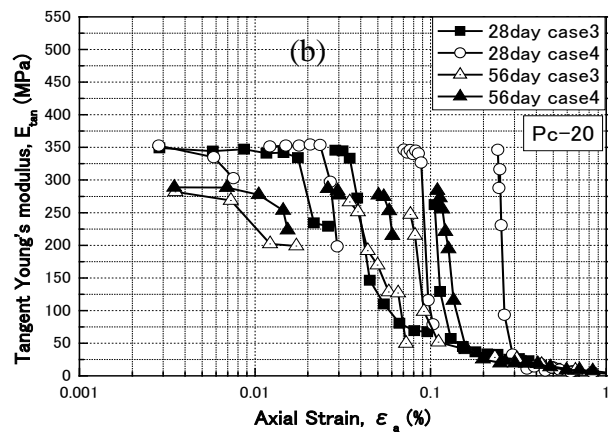
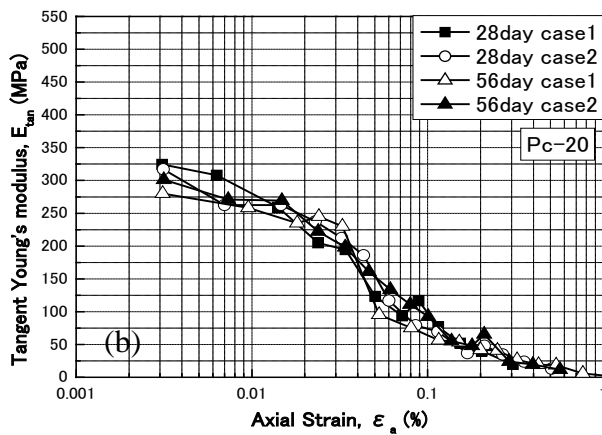
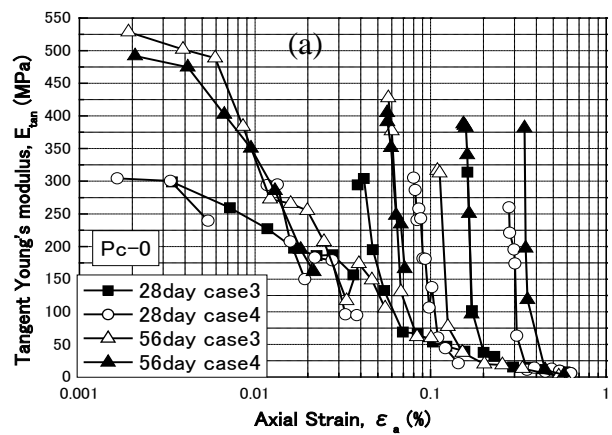
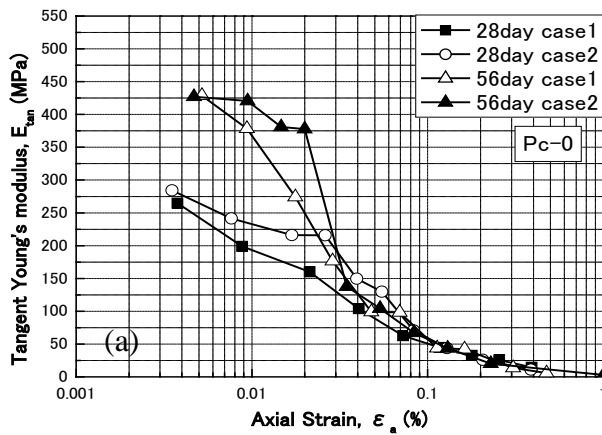


Figure 3.12 $E_{tan} \sim \log \epsilon_a$ relation for case 1, 2

Figure 3.13 $E_{tan} \sim \log \epsilon_a$ relation for case 3, 4

3.2.3 Summary

In order to investigate the effect of time-dependency on shear deformation characteristics of liquefied stabilized soil mixed with fiber material, a series of consolidated-undrained triaxial compression tests was performed under the four conditions of axial strain rate.

The following conclusions were derived based on test results.

1. Within this section, the maximum deviator stress, q_{\max} in $q\sim\varepsilon_a$ curve of LSS mixed with fibered material indicates similar value independently of curing days. However, in case of LSS without fibered material, there is a tendency to increase the initial stiffness as increasing of curing days.
2. Addition of fibered material to LSS increases the nonlinearity by an increase in the length of curing time, for this result it is considered to conduct further works in the coming time.
3. The range of indicating E_{\tan}/E_0 value of 1.0 tends to be larger on LSS mixed with fibered material. This is due to the reinforcing effect of the fibered material in LSS.
4. The rigidity during loading before the peak in $q\sim\varepsilon_a$ relationship increases temporarily in a large strain level after a creep stage and a change of strain rate independently of curing days.

3.3 STRENGTH AND DEFORMATION CHARACTERISTICS OF LSS PREPARED AT LABORATORY AND FIELD

In this section, a model ground was made by backfilling with LSS mixed with fiber material (an amount of 0, 20 kg/m³, respectively) into two pits constructed at the test field in campus. In parallel, the specimens of same batch were also molded and cured in laboratory. A series of consolidated undrained triaxial compression tests (CUB tests) were performed on both specimens prepared by trimming LSS retrieved from the model ground by block sampling (hereafter called in-situ LSS) and cured in laboratory (hereafter called indoor LSS) at the same curing time (28 and 56 days, respectively). The specimen was isotropically consolidated under the effective confined pressure of 98 kPa, and then, the specimen was sheared by triaxial compression under the condition at constant axial strain rate, constant deviator stress (partial creep), and changed strain rate during monotonic loading. Based on the test results, the difference in strength and deformation property of indoor LSS and in-situ LSS was discussed.

3.3.1 Test procedure

3.3.1.1 Test material and mixing method

Test material and mixing method were presented in 3.2.1.1 and 3.2.1.2, respectively.

3.3.1.2 Specimen preparation

After determining the liquidity of LSS following the steps as in 3.2.1.3, the fresh LSS mixed with fiber material amount of 0, 20 kg/m³, respectively then was poured into two pits constructed at the test field in campus, as shown in Figure 3.14. Before pouring, a nonwoven geotextile filter was set on to prevent seepage of LSS to original ground. After placing, the surface of LSS was covered with a polymer sheet and cured under outdoor condition. In parallel, the fresh LSS was also placed into mould of 5 cm in diameter and 10 cm in height, the top surface of the specimens was covered with a polymer film and were cured under air humidity and indoor temperature of 20±3°C. After curing time of 28 and 56 days, both the specimens prepared by trimming LSS retrieved from the model ground by block sampling method (in-situ LSS) and cured in laboratory (indoor LSS) were subjected to CUB tests.

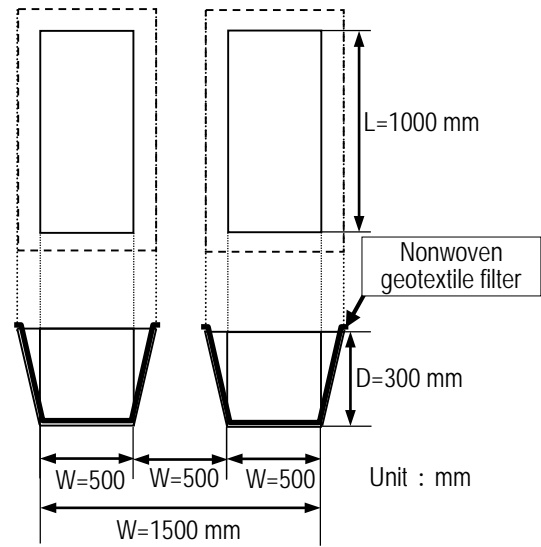


Figure 3.14 Schematic drawing of pits

(3) Test method

The outline of apparatus for triaxial compression tests is shown in Figure 3.3. The CUB tests were performed for both in-situ LSS and indoor LSS specimens at curing time of 28 and 56 days, respectively. The saturation of specimen was achieved by the double vacuum pressure method which the de-aired water flowed through specimen under a back pressure of 196 kPa. After isotropically consolidated during 12 hours under the effective confined pressure of 98 kPa, the specimen was sheared by triaxial compression. To investigate the strength and deformation property and the effect of creep on those of LSS mixed with fiber material, two cases of axial strain rate were used in this study as shown in Figure 3.15 and Figure 3.16. Case 1 was obtained by applying small unloading/reloading loops under monotonic loading process and axial strain rate of 0.054 %/min ($\dot{\epsilon}_0$). In case 2, creeps (C) were subjected during loading and

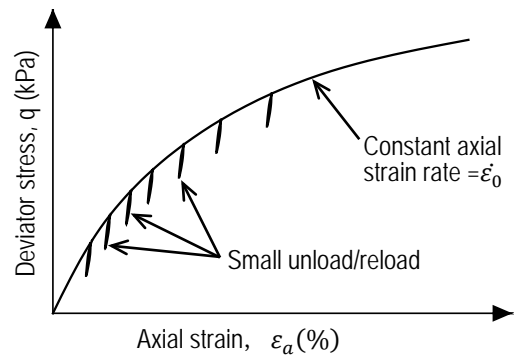


Figure 3.15 Case 1 of test condition

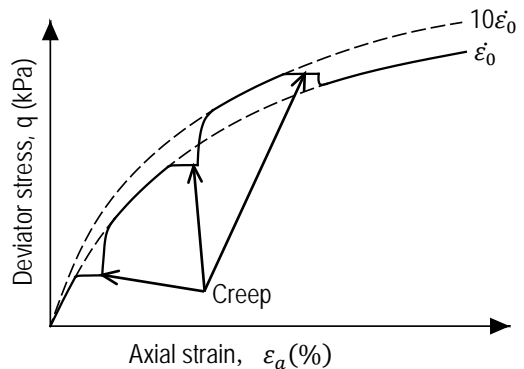


Figure 3.16 Case 2 of test condition

before a change of constant axial strain rate ($\dot{\epsilon}_0 \rightarrow C \rightarrow \dot{\epsilon}_0 \rightarrow C \rightarrow 10\dot{\epsilon}_0 \rightarrow C \rightarrow \dot{\epsilon}_0$). In addition, the change of axial strain rate was carried out in a range of about $\dot{\epsilon}_a=1\%$.

3.3.2 Test results and discussion

3.3.2.1 Relationship between deviator stress and axial strain

Figure 3.17 and Figure 3.18 show the relationship between the deviator stress q ($=\sigma_1 - \sigma_3$) and the axial strain ϵ_a in range of 0~2.0 % from the CUB tests under the confining pressure $\sigma'_c=98$ kPa for case 1 and case 2 of both indoor LSS and in-situ LSS mixed with fiber material amount of 0, 20 kg/m³ (Pc-0, 20) at 28 and 56 curing days, respectively. From the figures, as comparing the $q\sim\epsilon_a$ relation in each test of both 28 and 56 curing days, the maximum deviator stress, q_{max} of in-situ LSS specimens substantially tend to be larger than that of indoor LSS ones. It is caused to the factors of curing environment affecting the cementation into LSS. Then, it is considered that the onset of cementation was accelerated under outdoor curing condition compared to indoor curing condition, because the factors of curing environment humidity and temperature cannot be controlled. In addition, the q_{max} of both indoor LSS and in-situ LSS at 56 curing days is generally larger than that at 28 curing days. Therefore, it is considered that the strength of LSS mixed with fiber material increases as the increasing of curing time when LSS mixed with fiber material is used as a backfilling material at the sites. It is found from previous researches (Kohata et al., 2002, 2004, 2007; Ito et al.,

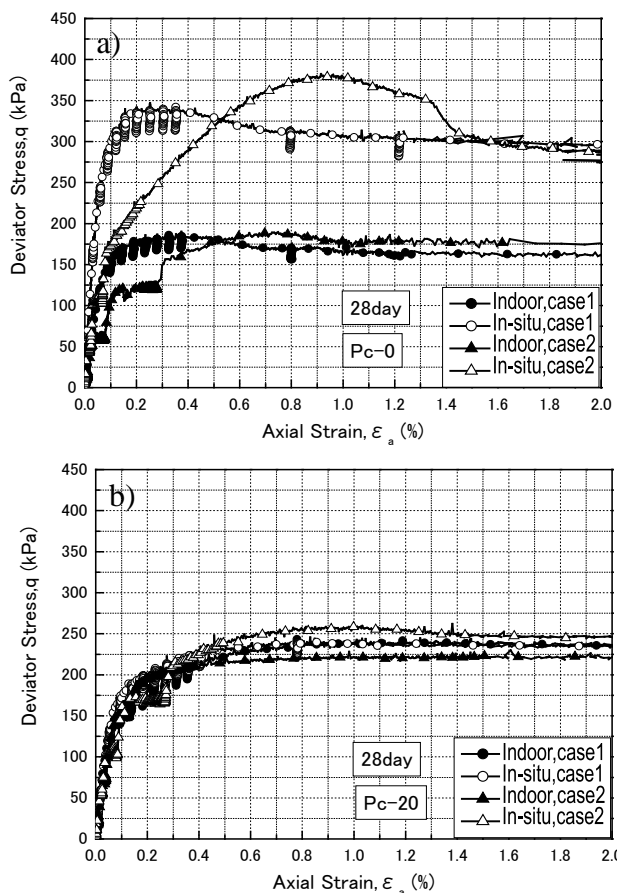


Figure 3.17 $q\sim\epsilon_a$ relations at 28 days

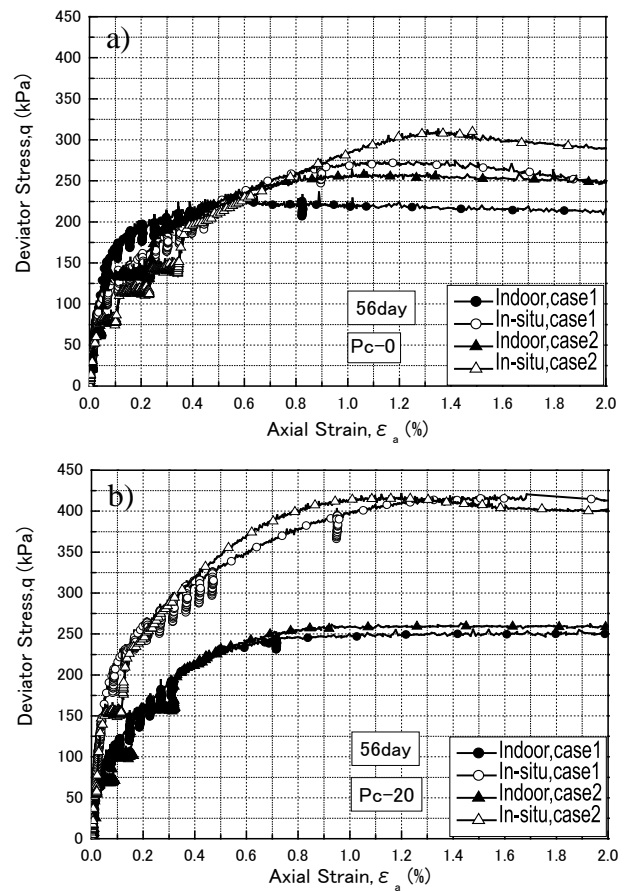


Figure 3.18 $q\sim\epsilon_a$ relations at 56 days

2011) that by the reinforcement effect, the brittle property of indoor LSS mixed with fiber material after the peak in $q\sim\varepsilon_a$ curve was improved. As shown in Figure 3.17(b) and Figure 3.18(b) the brittle property of both indoor LSS and in-situ LSS, Pc-20 after the peak in $q\sim\varepsilon_a$ curves is improved in comparison with pure LSS, Pc-0. For this reason, the application of LSS mixed with fiber material as a backfilling material to construction sites enables to create a ground with the improved ductile characteristic. Figure 3.17(b) indicates that the q_{max} of in-situ LSS, Pc-20 is smaller than that of other in-situ LSS, Pc-0. It seems that due to the addition of the fiber material, the cementation was considered to be delayed at early curing time.

3.3.2.2 Deformation property

a) Definition of Young's modulus

Figure 3.19 shows the definitions of various Young's moduli. The initial Young's modulus E_0 and The tangent Young's modulus E_{tan} are defined as in 3.2.2.2. The equivalent Young's modulus E_{eq} is obtained from small unloading/reloading loop during monotonic loading. Moreover, the E_{eq} in creep correction is calculated from slope of the lower limit point and the midpoint in line connecting the unloading point and the intersection of $q\sim\varepsilon_a$ curve in reloading. The E_{eq} indicates a changing of damage degree under the shearing (Kohata et al., 1997, 1999)

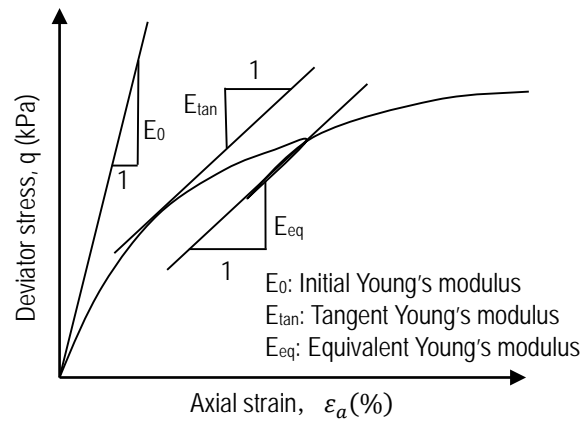


Figure 3.19 Definition of various Young's moduli

Figure 3.20 shows the relation of q_{max} and E_0 with curing days of in-situ LSS, Pc-0, 20, respectively. The results of in-situ LSS at 84 days with the same test conditions are shown here just for information. The values were obtained from the $q\sim\varepsilon_a$ curve of the CUB tests under the confining pressure of 98 kPa. From the figure, E_0 and q_{max} of Pc-0 is decreased at 56 days, but overall it tends to increase as at 84 days. In general, increase of the q_{max} of cement-treated soil with curing days has been known. However, q_{max} of

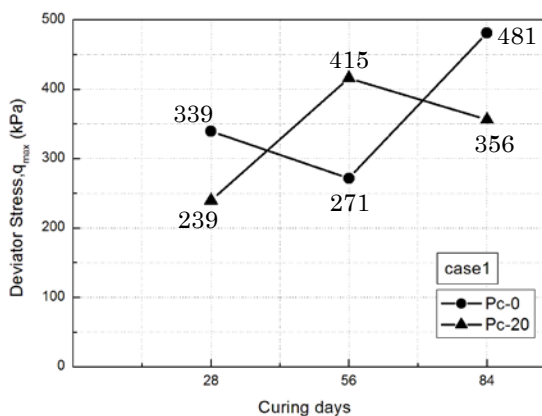


Figure 3.20a $q_{max}\sim$ curing days relations

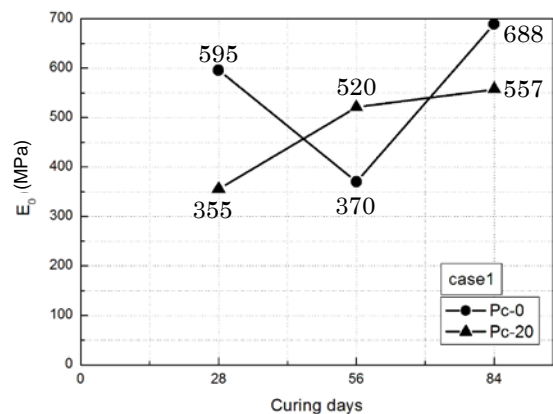


Figure 3.20b $E_0\sim$ curing days relations

Pc-20 decrease at 84 days though E_0 of one increases. Because the temperature of which the time is close to 84 curing days is below 0°C , it may be due to the effect of frost heave on the strength of specimen. For the reason, it is considered for further study.

b) Tangent Young's modulus E_{tan}

Figure 3.21 shows the relationship between E_{tan}/E_0 and q/q_{max} of both indoor LSS and in-situ LSS, Pc-0, 20, respectively at 28 days and 56 days for case 1. The values were obtained from the $q\sim\varepsilon_a$ curve of the CUB tests under the confining pressure of 98 kPa. In this Figure, reduction rate of E_{tan}/E_0 of indoor LSS and in-situ LSS shows a similar tendency in both Pc-0 and Pc-20 at 28 days and 56 days, respectively. Generally, cement-treated soil has been reported that nonlinearity of stress-strain curve decreases as increasing of curing days (JGS, 2005). However, within this study, a reduction rate of E_{tan}/E_0 of specimens at 56 days is larger than that at 28 days. Therefore, it seems that the nonlinearity increases as increasing of curing time. For this result, it is considered to conduct further works in the coming time.

Figure 3.22 shows the relationship between E_{tan}/E_0 and q/q_{max} for case 2. From the figure, it indicates that the E_{tan}/E_0 of both indoor LSS and in-situ LSS temporarily increase significantly immediately after applying a creep and initiating a new constant axial strain rate regardless of the curing days, thereafter, under loading the reduction of E_{tan}/E_0 tends to be larger. Thus, there is a tendency that the rigidity temporarily increases immediately after a creep is given. In addition, the range of indicating E_{tan}/E_0

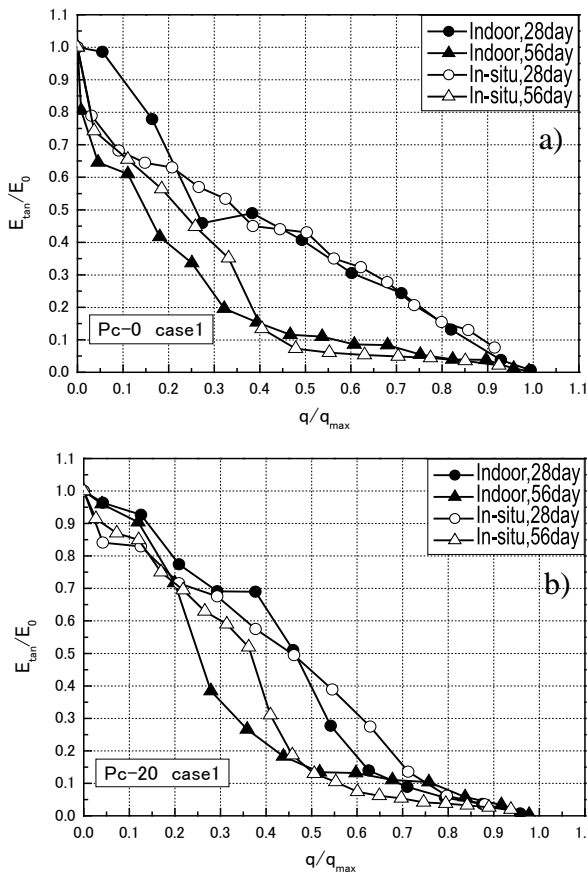


Figure 3.21 $E_{tan}/E_0\sim q/q_{max}$ relations for case 1

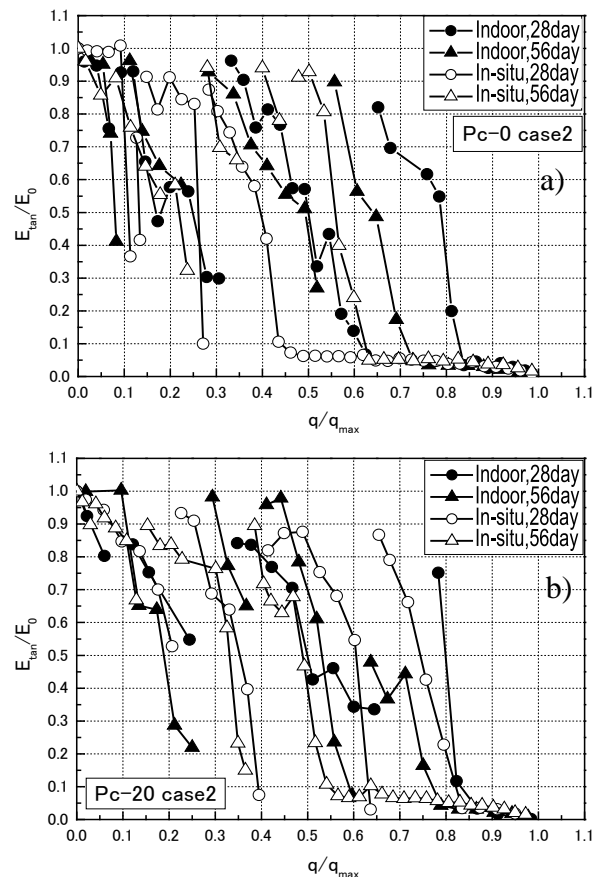


Figure 3.22 $E_{tan}/E_0\sim q/q_{max}$ relations for case 2

value of 1.0 tends to be larger in case of Pc-20 as compared with Pc-0. Therefore, it is considered that the range of linear in $q \sim \varepsilon_a$ relation becomes larger by the addition of the fiber material to LSS independent of the curing days. Then, it is found that due to the reinforcement effect by the addition of the fiber material, the linear range in $q \sim \varepsilon_a$ relation of in-situ LSS immediately after creep is increased.

c) Strain level-dependency of tangent Young's modulus, E_{tan}

Figure 3.23 shows the strain level-dependency of tangent Young's modulus E_{tan} until the peak in $q \sim \varepsilon_a$ curve of both indoor LSS and in-situ LSS, Pc-0, 20, respectively at 28 days and 56 days for case 1. It is seen that the initial stiffness of in-situ LSS tends to be larger than that of indoor LSS. However, a significant difference in strain level-dependency of E_{tan} is not found. Figure 3.24 shows the strain level-dependency of E_{tan} for case 2. In both indoor LSS and in-situ LSS, even in the range of large shear strain level, E_{tan} temporarily increase significantly immediately after a creep action. Moreover, in the case of Pc-20, a larger range of E_{tan} increasing nearly to the initial stiffness is observed. Thus, during loading before the peak in $q \sim \varepsilon_a$ relation, regardless of the curing days, the stiffness of LSS increases immediately after creep, even in the range of large shear strain level. By the addition of the fiber material, due to its reinforcing effect, the range that indicates large stiffness is increased.

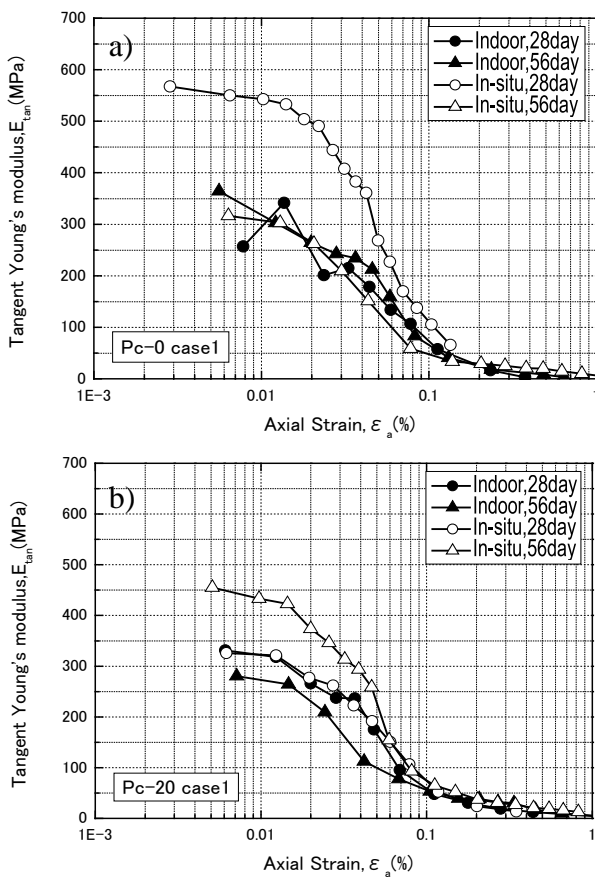


Figure 3.23 $E_{tan} \sim \log \varepsilon_a$ relations for case 1

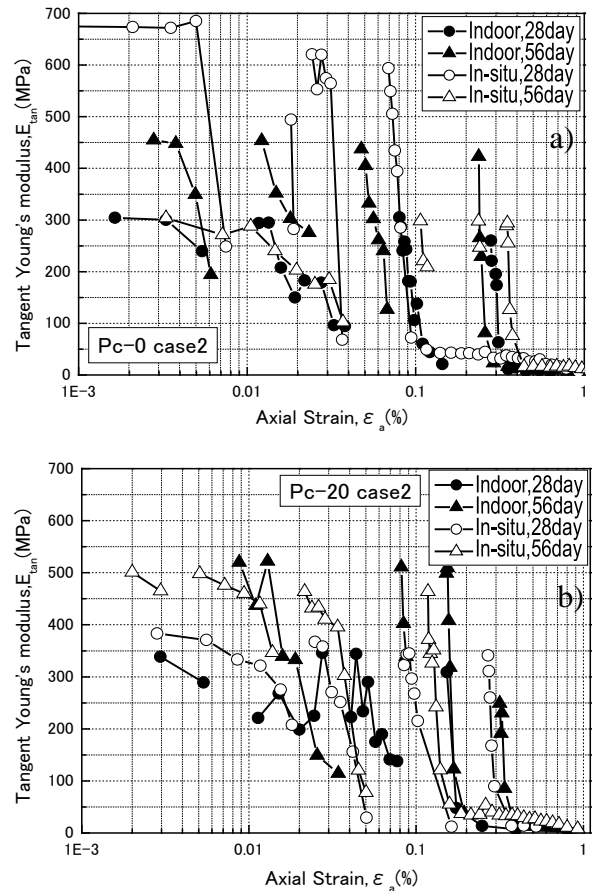


Figure 3.24 $E_{tan} \sim \log \varepsilon_a$ relations for case 2

d) Equivalent Young's modulus, E_{eq}

Figure 3.25 shows the relationship between E_{eq}/E_0 and q/q_{max} of both indoor LSS and in-situ LSS, Pc-0, 20, respectively at 28 days and 56 days. The values were obtained from the $q\sim\varepsilon_a$ curve of the CUB tests under the confining pressure of 98 kPa. In general, it has been reported that Young's modulus of cement-treated soil at small strain is independent of the confining pressure, thus, the E_{eq}/E_0 is considered indicating the change of damage degree under shearing. At first stage, the shearing cause soil specimen to break locally, and finally the soil specimen is entirely destroyed as the shear band is formed by the accumulation of the local destructions. This is considered that the cementation or microstructure between particles of the soil is damaged, and then such damages cause the changes of elasticity. It is seen from the figure in the case of indoor LSS that overall the reduction rate of E_{eq}/E_0 of Pc-20 tends to be smaller than that of Pc-0. Thus, the fiber material inside specimen is suggested mitigating the local damage caused by shearing. However, in the case of in-situ LSS, the reduction rate of E_{eq}/E_0 of Pc-20 at 56 curing days is large. It is probably due to the influence of the disturbance at the time of sampling and curing environment, which causes remarkably damage for the sample under shearing. For this result, it is considered to conduct further works in the coming time.

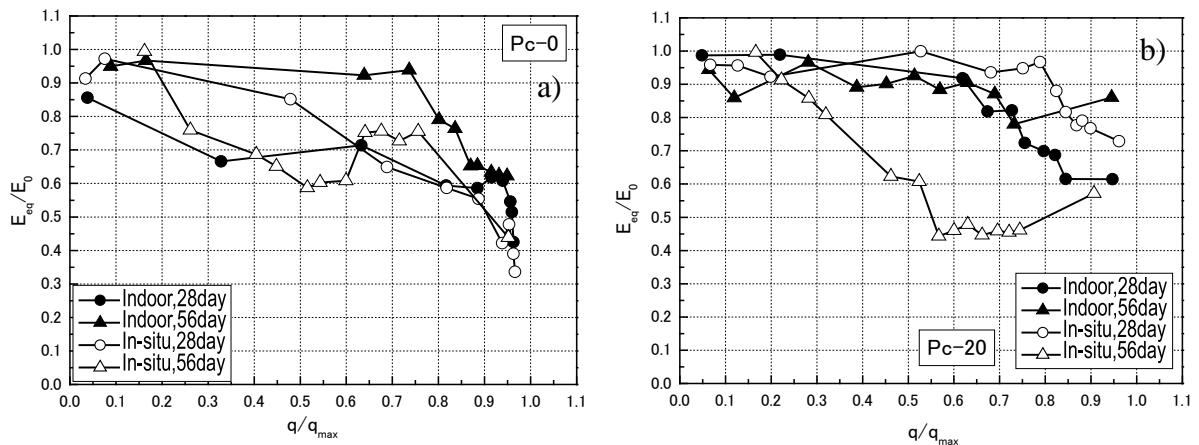


Figure 3.25 $E_{eq}/E_0 \sim q/q_{max}$ relations

3.3.3 Summary

In order to evaluate the strength and deformation properties of Liquefied Stabilized Soil mixed with fiber material cured in laboratory and at field, a series of consolidated-undrained triaxial compression tests was performed under the two conditions of axial strain rate for both specimens retrieved from the model ground by block sampling and cured in laboratory at curing time of 28 and 56 days.

The following conclusions were derived based on test results.

1. Within this section, the maximum deviator stress, q_{max} in $q\sim\varepsilon_a$ curve of LSS mixed with fiber material cured at field substantially tend to be larger than that cured in laboratory. Moreover, by the addition of the fiber material, the brittle property of LSS cured in field after the peak is improved.

2. The $E_{tan}/E_0 \sim q/q_{max}$ relation of both LSS cured in laboratory and at field shows relatively similar tendency. In addition, the nonlinearity in $q \sim \varepsilon_a$ relation of LSS due to its reinforcing effect is weakened.
3. It is considered that the linear region on $q \sim \varepsilon_a$ relation increases immediately after creep due to reinforcing effect when the fiber material is mixed in LSS prepared at field.
4. It is suggested that the application of LSS mixed with fiber material as a backfilling material to construction sites enables to create a ground with the improved ductile characteristic, although it needs to conduct more study.

REFERENCES

Tatsuoka, F., Ishihara, M., Di Benedetto, H. and Kuwano, R. (2002): Time-dependent shear deformation characteristics of geomaterials and their simulation, *Soils and Foundations*, Vol.42, No.2, pp.103-129.

Di Benedetto, H., Tatsuoka, F. and Ishihara, M. (2002): Time-dependent deformation characteristics of sand and their constitutive modelling, *Soils and Foundations*, Vol.42, No.2, pp.1-22.

Koyama, Y., Kohata, Y. and Omura, S. (2012): Study on the effect of time-dependency on the strength and deformation characteristics of liquefied stabilized soil mixed with fibered material, *Japanese Geotechnical Society Hokkaido Branch Technical Report Papers*, Vol.52, pp.56-62 (in Japanese).

Kohata, Y., Ito, K. and Koyama, Y. (2011): Impact of cement based solidifying material on the mechanical characteristics of liquefied stabilized soil mixed with fibered material, *Japanese Geotechnical Society Hokkaido Branch Technical Report Papers*, Vol.51, pp.131-136 (in Japanese).

Goto, S., Tatsuoka, F., Shibuya, S., Kim, Y. S. and Sato, T. (1991): A simple gauge for local small strain measurements in the laboratory, *Soils and Foundations*, Vol.31, No.1, pp 169-180.

Japanese Geotechnical Society (2005): Committee Report Chapter 2, 2.1, 2.2 on test methods and physical properties of cement-modified soil, *Symposium papers collection*, pp.2-22, on survey, design, construction and properties evaluation methods of solidifying stabilized soil using cement and cement-modified soil (in Japanese).

Kohata, Y., Tatsuoka, F., Wang, L., Jiang, L. G., Hoque, E., and Kodaka, T. (1997): Modelling the non-linear deformation properties of stiff geomaterials, *Géotechnique*, Vol.47, No.3, pp.563-580.

Kohata, Y., Jiang, L. G., Murata, O., and Tatsuoka, F. (1999): Elastic-properties-based modelling of non-linear deformation characteristics of gravels, *Proc. of the second Inter. Symposium on Pre-Failure Deformation Characteristics of Geomaterials-IS Torino 99*, pp.533-539.

Kohata, Y., Fujikawa, T., Ichihara, D., Kanda, M., and Murata, O. (2002): Strength

and deformation properties of fibered material mixed in liquefied stabilized soil obtained from uniaxial compression test, *Proc. of the 36th Japan National Conf. on Geotech. Eng.*, pp.635-636 (in Japanese).

Kohata, Y., and Tsushima, H. (2004): Effect of fibered material mixing in liquefied stabilized soil on the triaxial shear characteristics, *Proc. of the 39th Japan National Conf. on Geotech. Eng.*, pp.721-722 (in Japanese).

Kohata, Y., Ichikawa, M., Nguyen, C. Giang., and Kato, Y. (2007): Study of damage characteristics of liquefied stabilized soil mixed with fibered material due to triaxial shearing, *Geosynthetics Engineering Journal*, Vol.22, pp.55-62 (in Japanese).

Ito, K., Kohata, Y., and Koyama, Y. (2011): Influence of additive amount of cement solidification agent on mechanical characteristics of Liquefied Stabilized Soil mixed with fibered material, *Japanese Geotechnical Society Hokkaido Branch Technical Report Papers*, Vol.51, pp.131-136 (in Japanese).